

A new way to test the WIMP dark matter models

Wei Cheng,^{1,2} Yuan He,¹ Jin-Wang Diao,¹ Yu Pan,^{†,1} Jun Zeng^{†,3} and Jia-Wei Zhang⁴

¹*School of Science, Chongqing University of Posts and Telecommunications, Chongqing 400065, P. R. China*

²*State Key Laboratory of Theoretical Physics, Institute of Theoretical Physics, Chinese Academy of Sciences, Beijing, 100190, P.R. China*

³*Department of Physics, Chongqing University, Chongqing 401331, P.R. China*

⁴*Department of Physics, Chongqing University of Science and Technology, Chongqing 401331, P. R. China*

[†]Corresponding authors:

E-mail: panyu@cqupt.edu.cn, zengj@cqu.edu.cn

ABSTRACT: In this paper, we investigate the possibility of testing the weakly interacting massive particle (WIMP) dark matter (DM) models by applying the simplest phenomenological model which introduces an interaction term between dark energy (DE) and WIMP DM, i.e., $Q = 3\gamma_{DM}H\rho_{DM}$. In general, the coupling strength γ_{DE} is close to 0 due to the interaction between DE and WIMP DM is very weak, thus the effect of γ_{DE} on the evolution of Y associated with DM energy density can be safely ignored. Meanwhile, our numerical calculation also indicates that $x_f \approx 20$ is associated with DM freeze-out temperature, which is the same as the vanishing interaction scenario. As for DM relic density, it will be magnified by $\frac{2-3\gamma_{DM}}{2}[2\pi g_* m_{DM}^3/(45s_0 x_f^3)]^{\gamma_{DM}}$ times, which provides a new way for us to test WIMP DM models. As an example, we analyze the case in which WIMP DM is a scalar DM. (SGL+SNe+Hz) and (GRBs+SNe+BAO+CMB) cosmological observations will give out $\gamma_{DM} = 0.134_{-0.069}^{+0.17}$ and $\gamma_{DM} = -0.0047 \pm 0.0046$, respectively. After further considering the constraints from both the DM direct detection experiment and DM relic density, we observe that the allowed parameter space of the scalar DM model will be completely excluded for the former cosmological observations, while it will increase for the latter ones. Those two cosmological observations lead to a paradoxical conclusion. Thus we wish the more accuracy of the cosmological observation can be obtained in the near future to test the WIMP DM models.

Contents

1	Introduction	1
2	Dark energy and WIMP dark matter interaction models	2
3	Observational Data in Cosmology	3
4	WIMP dark matter relic density	5
5	Example – Scalar dark matter being the WIMP dark matter	6
5.1	Scalar dark matter model	6
5.2	Cosmology observable constraint on γ_{DM}	7
5.3	WIMP DM relic density	9
5.4	DM direct detection	11
6	Summary	13

1 Introduction

Dark energy (DE) and dark matter (DM), which are the main parts of the energy content of the universe, have been firmly established by numerous astronomical and cosmological observations [1–5]. More specifically, the cosmic microwave background (CMB) anisotropies have inferred the abundance of DM and DE with remarkable precision at $(26.0 \pm 0.5)\%$ [6, 7] and $(68.89 \pm 0.56)\%$ [8] respectively. The usual strategy of particle physicists to deal with the DM is to extend the standard model (SM) of particle physics by adding a new particle that interacts with the SM particles. Based on this interaction, physicists have conducted indirect detection [9–13], direct detection [14–17], and collider detection [18–21] for testing DM models.

There are numerous literatures devoting to explore the interaction between DE and DM to relieve the coincidence problem [22–38]. More specifically, in Ref. [39], the interaction type between DM and DE is set as $Q = 3H\gamma_m\rho_m$. After considering the limits from the combination of cosmological data (GRBs+SNe+BAO+CMB), the coupling strength of DM and DE can be obtained, i.e., $\gamma_m = -0.0047 \pm 0.0046$ in 1σ errors, which indicates the energy of DM transfer to that of DE slightly. In Ref. [40], the interaction between DE and DM (baryonic substances) is set as $3H\gamma_c\rho_c$ ($3H\gamma_b\rho_b$). Taking the bounds from the combination of cosmological data (SNe+BAO+Planck+H(Z)), one can obtain $\gamma_c = 0.0078 \pm 0.0045$ and $\gamma_b = 0.0030^{+0.0255}_{-0.0125}$ in 1σ errors, while using the bounds from the combinations of cosmological data (SNe+BAO+WMAP9+H(z)), one can get $\gamma_c = 0.0068^{+0.0043}_{-0.0042}$

and $\gamma_b = 0.0025^{+0.0235}_{-0.0115}$ in 1σ errors. If one sets $\gamma_b = 0$, then $\gamma_c = 0.0095 \pm 0.0031$ in 1σ errors within the bounds from the combinations of cosmological data (SNe+BAO+Planck+H(z)), while $\gamma_c = 0.0081 \pm 0.0031$ in 1σ errors within the bounds from the combinations of cosmological data (SNe+BAO+WMAP9+H(z)). All predictions of Ref. [40] indicate $\gamma_c > 0$, which means the energy of DE is slightly transferring to that of DM. These two references however imply that cosmological data cannot completely exclude the interaction between DE and DM, and different cosmological data may lead to different energy of transferring predictions between DE and DM.

Motivated by the method of DM Models detection which is based on the interaction between the SM particle and new particles [41–46], in this paper, we will attempt to develop an alternative DM models verification method based on the added interaction between DM and DE, in which we will restrict ourselves to the Weakly Interacting Massive Particle (WIMP) DM. Specifically, we studied the simplest type of interaction between DE and WIMP DM, namely $Q = 3\gamma_{DM}H\rho_M$. We deduced the WIMP DM relic density that can be used to examine the WIMP DM models with help of the DM detection experiments.

As an example, we will describe the WIMP DM as a real scalar particle which is the simplest Higgs-portal DM model and has had been comprehensively revisited [47–54]. After considering the WIMP DM relic density, we find that the parameter space of the scalar model will increase with $\gamma_{DM} < 0$, and the smaller γ_{DM} , the larger increased parameter space of the model; while the parameter space will shrink with $\gamma_{DM} > 0$, and the larger γ_{DM} , the larger excluded parameter space of this model.

The remaining parts of this paper are organized as follows. In Sec. 2, we construct the DE and WIMP DM models with a interaction term $Q = 3\gamma_{DM}H\rho_M$. In Sec. 3, three observational data in Cosmology are described for further constraining the coupling strength γ_{DM} . In Sec. 4, the WIMP DM relic density in the new models are calculated. As an example, a scalar DM being the WIMP DM is investigated in detail in Sec. 5. Finally, we will briefly summarize in Sec. 6.

2 Dark energy and WIMP dark matter interaction models

The energy evolution of DE and matter can be described as follows [40, 55]:

$$\begin{aligned}\dot{\rho}_{DE} + 3H(\rho_{DE} + P_{DE}) &= -Q, \\ \dot{\rho}_M + 3H\rho_M &= Q.\end{aligned}\tag{2.1}$$

where ρ_{DE} and ρ_M are the DE and matter energy respectively. The interaction term Q describes the interchange of energy with each other, but there is a vanishing interaction between them when $Q = 0$. Note that those two energies meet the total energy conservation equation: $\dot{\rho}_{tot} + 3H(\rho_{tot} + P_{tot}) = 0$.

We will further divide the matter energy into DM and the usual standard model matter, i.e. $\rho_M = \rho_{DM} + \rho_{SM}$. If the DM is the WIMP, then the evolution of ρ_{DM} can be written as

follows:

$$\dot{\rho}_{DM} + 3H\rho_{DM} = Q_{DM} + \frac{\langle\sigma v\rangle}{m_{DM}}(\rho_{DM,eq}^2 - \rho_{DM}^2), \quad (2.2)$$

where $\langle\sigma v\rangle$ is the WIMP DM thermal average cross section, and $\rho_{DM,eq}$ represent the WIMP DM energy of thermal equilibrium state.

As extensively considered in the literature, we will consider the usual scenario interaction term $Q = 3\gamma_{DM}H\rho_M$ and assume $Q_{DM} = 3\gamma_{DM}H\rho_{DM}$. When $\gamma_{DM} < 0$, the energy is transferred from WIMP DM to DE; while for $\gamma_{DM} > 0$, the energy is transferred from DE to WIMP DM, which will affect the feasible parameters of the WIMP DM model. Specifically, the feasible parameters of the WIMP DM model will be shrunken for the case $\gamma_{DM} > 0$, while it will be increased for the case $\gamma_{DM} < 0$. Furthermore, the standard Λ CDM model without interaction between DE and matter is characterized by $Q = 0$, while $Q \neq 0$ represents the non-standard cosmology with interaction between DE and matter.

With the above Eqs. (2.2) at hands, we can establish a relation between the coupling strength γ_{DM} and the thermal average cross section of WIMP DM through its relic density. As the cosmology observations make a constrain for the coupling strength γ_{DM} through the Eq. (2.1), we can also establish a relation between the cosmology observations and the thermal average cross section of WIMP DM. We will discuss it in detail in the following parts.

3 Observational Data in Cosmology

In this section, we will introduce three kinds of observational data in cosmology to constrain the γ_{DM} interaction dark energy model parameters, i.e., 130 updated galaxy-scale strong gravitational lensing sample (SGL) [56] with redshift from 0.197 to 2.834, Hubble parameter data (Hz) [57], and Pantheon 1048 Ia supernovae sample (SNe) discovered by the Pan-STARRS1 Medium Deep Survey [58].

Considering the influence of some unknown system errors on the SGL data, Chen et al. compiled 161 galaxy-scale strong gravitational lensing sample systems which include the gravitational lensing and stellar velocity dispersion measurements. They selected those samples from early-type galaxies with $E/S0$ morphologies with strict criteria to satisfy the assumption of spherical symmetry on the lens mass model. In which, they discuss the slope of the total mass density profile γ considering three parameterizations ($\gamma = \gamma_0$, $\gamma = \gamma_0 + \gamma_z \times z_l$ and $\gamma = \gamma_0 + \gamma_z \times z_l + \gamma_s \times \log \tilde{\Sigma}$), the luminosity density slope δ with an observable parameter for each lens and the orbit anisotropy parameter β treated as a nuisance parameter and marginalized over with a Gaussian prior $\beta = 0.18 \pm 0.13$ [56]. Moreover, because of high-resolution HST imaging data needed, they finally chose 130 galaxy-scale strong gravitational lensing data from 161 samples, which are separately from the Sloan Lens ACS(SLACS) and others surveys. The specific selection methods can be found in the literature [56].

When considering the effect of aperture size on the velocity dispersion of the lens galaxy, a more appropriate choice for the radius is $R_{\text{eff}}/2$ with R_{eff} being the half-light radius of the

lens galaxy, because R_{eff} matches the Einstein radius well [59]. Choose $R_{\text{eff}}/2$ as the radius to get the velocity dispersion σ_{e2} , according to the regulations, the observational expression of velocity dispersion is as follows:

$$\sigma_{\text{obs}} \equiv \sigma_{e2} = \sigma_{ap} [\theta_{\text{eff}} / (2\theta_{ap})]^\eta, \quad (3.1)$$

where σ_{ap} is velocity dispersion, $\theta_{\text{eff}} = R_{\text{eff}}/D_l$, the correction factor $\eta = -0.066 \pm 0.035$ [60], and $\theta_{ap} \approx 1.025 \times \sqrt{(\theta_x \theta_y / \pi)}$ with θ_x and θ_y being the angular sizes of width and length of the rectangular aperture respectively [61].

The total error of the actual velocity dispersion is:

$$(\Delta\sigma_{\text{tot}})^2 = (\Delta\sigma_{\text{stat}})^2 + (\Delta\sigma_{\text{sys}})^2 + (\Delta\sigma_{\text{AC}})^2, \quad (3.2)$$

where $\Delta\sigma_{\text{stat}}$, propagated from the measurement error of σ_{ap} , is the statistical error, $\Delta\sigma_{\text{sys}}$ is systematic error, and the error $\Delta\sigma_{\text{AC}}$ is propagated from the uncertainty of η due to the aperture correction.

The theory of velocity dispersion can be expressed as:

$$\sigma_{th} = \sqrt{\frac{c^2}{2\sqrt{\pi}} \frac{D_s}{D_{ls}} \theta_E \frac{3-\delta}{(\xi-2\beta)(3-\xi)} F(\gamma, \delta, \beta) \left(\frac{\theta_{\text{eff}}}{2\theta_E}\right)^{(2-\gamma)}}, \quad (3.3)$$

where D_{ls} is the angular diameter distance between lens and source, D_s is that between observer and source, which are dependent on the cosmological model. The cosmological model enters into the theoretical observable not through a distance measure directly, but rather through a distance ratio: $\frac{D_s(z_s; \mathbf{p}, H_0)}{D_{ls}(z_l, z_s; \mathbf{p}, H_0)}$. The expressions for both $D_s(z_s; \mathbf{p}, H_0)$ and $D_{ls}(z_l, z_s; \mathbf{p}, H_0)$ are as follows:

$$D_s(z_s; \mathbf{p}, H_0) = \frac{c}{H_0(1+z_s)} \int_0^{z_s} \frac{dz}{E(z; \mathbf{p})}, \quad (3.4)$$

$$D_{ls}(z_l, z_s; \mathbf{p}, H_0) = \frac{c}{H_0(1+z_s)} \int_{z_l}^{z_s} \frac{dz}{E(z; \mathbf{p})}, \quad (3.5)$$

where $E(z; \mathbf{p})$ is the cosmological background of the γ_{DM} model that has the following form:

$$E^2(z; \mathbf{p}) = \frac{w_x \Omega_m}{\gamma_{DM} + w_x} (1+z)^{3(1-\gamma_{DM})} + \left(1 - \frac{w_x \Omega_m}{\gamma_{DM} + w_x}\right) (1+z)^{3(1+w_x)} \quad (3.6)$$

where \mathbf{p} is the model parameters, i.e., $\mathbf{p} = (\Omega_m, w_x, \gamma_{DM})$.

The function $F(\gamma, \delta, \beta)$ in the Eq.(3.3) can be expressed as:

$$F(\gamma, \delta, \beta) = \left[\frac{\Gamma[(\xi-1)/2]}{\Gamma(\xi/2)} - \beta \frac{\Gamma[(\xi+1)/2]}{\Gamma[(\xi+2)/2]} \right] \frac{\Gamma(\gamma/2)\Gamma(\delta/2)}{\Gamma[(\gamma-1)/2]\Gamma[(\delta-1)/2]}. \quad (3.7)$$

where $\xi = \gamma + \delta - 2$. In this paper, we consider the dependence of γ on lens redshift z_l and the dependence of redshift on surface mass density (i.e., P3 in the literature[56]). The expression of γ is as follows:

$$\gamma = \gamma_0 + \gamma_z \times z_l + \gamma_s \times \log \tilde{\Sigma}, \quad (3.8)$$

where $\tilde{\Sigma}$ is the surface mass density,

$$\tilde{\Sigma} = \frac{(\sigma_{obs}/100 \text{ kms}^{-1})^2}{R_{\text{eff}}/10h^{-1} \text{ kpc}} \quad (3.9)$$

h is from the Hubble constant $H_0 = 100h \text{ km}^{-1}\text{Mpc}^{-1}$.

In addition, we also consider the latest Pantheon supernova sample [58]

$$\mu = M + 5 \log \frac{d_L}{\text{pc}} + 25, \quad (3.10)$$

where

$$d_L = \frac{(1+z)}{H_0} \int_0^z \frac{dz'}{E(z')}. \quad (3.11)$$

Finally, the 31 Hubble parameter (Hz) samples from the differential age method are also used [57].

4 WIMP dark matter relic density

The evolution of DM can be described by:

$$\dot{\rho}_{DM} + 3H\rho_{DM} = 3\gamma_{DM}H\rho_{DM} + \frac{\langle\sigma v\rangle}{m_{DM}}(\rho_{DM,eq}^2 - \rho_{DM}^2), \quad (4.1)$$

where $\rho_{DM} = m_{DM}n_{DM}$ with n_{DM} being the DM number density. The above evolution of DM equation contains the core information of DM, such as the freeze-out parameter $x_f = m_{DM}/T$ with T being the DM freeze-out temperature and the DM relic density. In the following, we will go through the derivation of these quantities in detail in this new model [62].

By making a substitution $x = m_{DM}/T$ and $Y = n_{DM}S^{\gamma_{DM}-1}$ with S being the entropy of the universe, we can rewrite Eq. (4.1) with the help of relation $dS(T)/dt + 3S(T)H = 0$ and $\langle\sigma v\rangle = \langle\sigma v\rangle_0 x^{-n}$, as follows:

$$\frac{dY}{dx} = \frac{\langle\sigma v\rangle_0 x^{3\gamma_{DM}-n-2}}{H(m)S(m)^{\gamma_{DM}-1}}(Y_{eq}^2 - Y^2), \quad (4.2)$$

where $H(m) = Hx^2$ and $S(m) = S(T)x^3$.

For the further study, we set $y = \frac{\langle\sigma v\rangle_0 n_{DM} s^{\gamma_{DM}-1}}{H(m)S(m)^{\gamma_{DM}-1}}$, thus $y_{eq} = \frac{\langle\sigma v\rangle_0 n_{DM,eq} s^{\gamma_{DM}-1}}{H(m)S(m)^{\gamma_{DM}-1}}$ with $n_{DM,eq} = g(\frac{mT}{2\pi})^{3/2} \exp(-m/T)$. We can further transform Eq. (4.1) as:

$$\frac{dy}{dx} = \frac{1}{x^{3-3\gamma_{DM}}}(y_{eq}^2 - y^2). \quad (4.3)$$

The interaction strength γ_{DM} between DE and DM, though generally small, will be set to $\gamma_{DM} < |0.05|$ to test the x_f . Taking the usual inputs¹, we plot Y as a function of x in Fig. 4. We find that x_f almost doesn't change in $\gamma_{DM} < |0.05|$, i.e., $x_f \approx 20$.

¹DM mass is $m_{DM} = 1000 \text{ GeV}$, reduced Planck mass is $M_{Pl} = (8\pi G)^{-1/2} = 2.44 \times 10^{18} \text{ GeV}$, the number of degrees of freedom for the field is $g_* = 100$, and the cross section is $\langle\sigma v\rangle_0 = 10^{-10} \text{ GeV}^{-2}$.

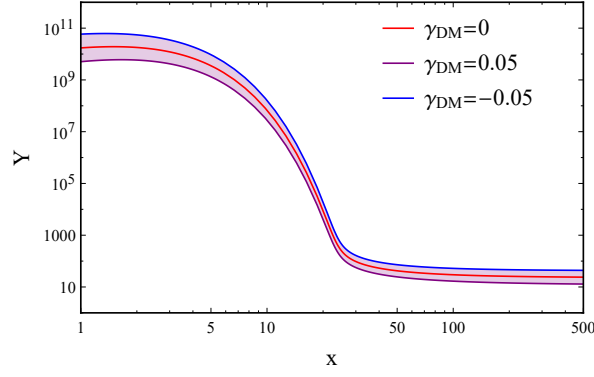


Figure 1. The plot of Y by x for several values of γ_{DM} .

As the WIMP DM relic density is given by:

$$\Omega = \frac{\rho_{DM_0}}{\rho_{crit}} \quad (4.4)$$

where the critical energy density $\rho_{crit} = \frac{3H_0}{8\pi G_N}$ and the energy density of DM today can be expressed as follows:

$$\rho_{DM_0} = m_{DM} Y_\infty s_0^{1-\gamma_{DM}}, \quad (4.5)$$

where $Y_\infty = \frac{H(m)S(m)\gamma_{DM}^{-1}}{\langle\sigma v\rangle_0} (n+1-3\gamma_{DM}) x_f^{n+1-3\gamma_{DM}}$, which can be obtained by solving the Eq. (4.2), and the entropy of the universe today is $S_0 = 2890 \text{ cm}^{-3}$.

Finally, the WIMP DM relic density can be obtained with $n = 1$ as follows:

$$\Omega h^2 = 0.169 \times x_f \sqrt{\frac{100}{g_*} \frac{10^{-10} \text{ GeV}^{-2}}{\langle\sigma v\rangle} \frac{2-3\gamma_{DM}}{2} \left(\frac{2\pi g_* m_{DM}^3}{45 S_0 x_f^3} \right)^{\gamma_{DM}}}. \quad (4.6)$$

5 Example – Scalar dark matter being the WIMP dark matter

5.1 Scalar dark matter model

Let us firstly discuss the Higgs potential with a real scalar DM, which can be written as[53]:

$$V(\Phi, \mathcal{S}) = -\mu_h^2 |\Phi|^2 + \lambda_h |\Phi|^4 + \frac{1}{2} \mu_{\mathcal{S}}^2 \mathcal{S}^2 + \frac{1}{2} \lambda_{\mathcal{S}} \mathcal{S}^4 + \frac{1}{2} \lambda_{h\mathcal{S}} |\Phi|^2 \mathcal{S}^2, \quad (5.1)$$

where Φ and \mathcal{S} are the SM Higgs and the real scalar DM, respectively. The interaction between DM sector and SM Higgs is described by the last term, and the coupling constant $\lambda_{h\mathcal{S}}$ reflect the strength of this interaction. The cubic term of \mathcal{S} is eliminated due to the even Z_2 parity symmetry of the real scalar DM.

Parameters	1 σ	2 σ
Ω_m	$0.445^{+0.15}_{-0.076}$	$0.445^{+0.19}_{-0.23}$
ω_x	$-1.59^{+0.54}_{-0.35}$	$-1.59^{+0.71}_{-0.82}$
γ_{DM}	$0.134^{+0.17}_{-0.069}$	$0.134^{+0.23}_{-0.32}$
H_0	71.54 ± 0.39	$71.54^{+0.78}_{-0.74}$
γ_0	1.237 ± 0.067	$1.237^{+0.15}_{-0.15}$
γ_z	-0.218 ± 0.074	$-0.218^{+0.14}_{-0.15}$
γ_s	0.652 ± 0.055	$0.652^{+0.11}_{-0.11}$

Table 1. The best values (Ω_m , ω_x , γ_{DM} , H_0 , γ_0 , γ_z , γ_s) and their 2σ errors of the γ_{DM} model parameters are obtained by using SGL+SNe+Hz observational data combination.

After the electroweak symmetry spontaneously breaks, the dark sector of Eq. (5.1) can be written as,

$$V(h, \mathcal{S}) = \frac{m_{\mathcal{S}}^2}{2} \mathcal{S}^2 + \frac{\lambda_{\mathcal{S}}}{2} \mathcal{S}^4 + \frac{\lambda_{h\mathcal{S}v}}{2} \mathcal{S}^2 h + \frac{\lambda_{h\mathcal{S}}}{4} \mathcal{S}^2 h^2, \quad (5.2)$$

where the square of DM mass is $m_{\mathcal{S}}^2 = \mu_{\mathcal{S}}^2 + \lambda_{h\mathcal{S}}v^2/2$ with the electroweak scale $v \simeq 246$ GeV.

5.2 Cosmology observable constraint on γ_{DM}

The parameters of the γ_{DM} model are constrained by using (SGL+SNe+Hz) sample combination through Markov chain Monte Carlo(MCMC) method [63], and fitted by the minimum likelihood method of χ^2 . The final χ_{All}^2 is given by the following function:

$$\chi_{All}^2 = \chi_{SGL}^2 + \chi_{SNe}^2 + \chi_{Hz}^2. \quad (5.3)$$

where χ_{SGL}^2 , χ_{SNe}^2 , and χ_{Hz}^2 can be expressed as follows:

$$\chi_{SGL}^2 = \sum_{i=1}^{130} \left(\frac{\sigma_{th} - \sigma_{obs}}{\Delta\sigma_{tot}} \right)^2, \quad (5.4)$$

$$\chi_{SNe}^2 = \sum_{i=1}^{1048} \left(\frac{\mu_{th} - \mu_{obs}}{\sigma_{\mu}} \right)^2, \quad (5.5)$$

$$\chi_{Hz}^2 = \sum_{i=1}^{31} \left(\frac{Hz_{th} - Hz_{obs}}{\sigma_{Hz}} \right)^2. \quad (5.6)$$

The best values of each parameters (Ω_m , ω_x , γ_{DM} , H_0 , γ_0 , γ_z , γ_s) and their 2σ error results are shown in Table.1. The 2D contour line is shown in Fig.5.2.

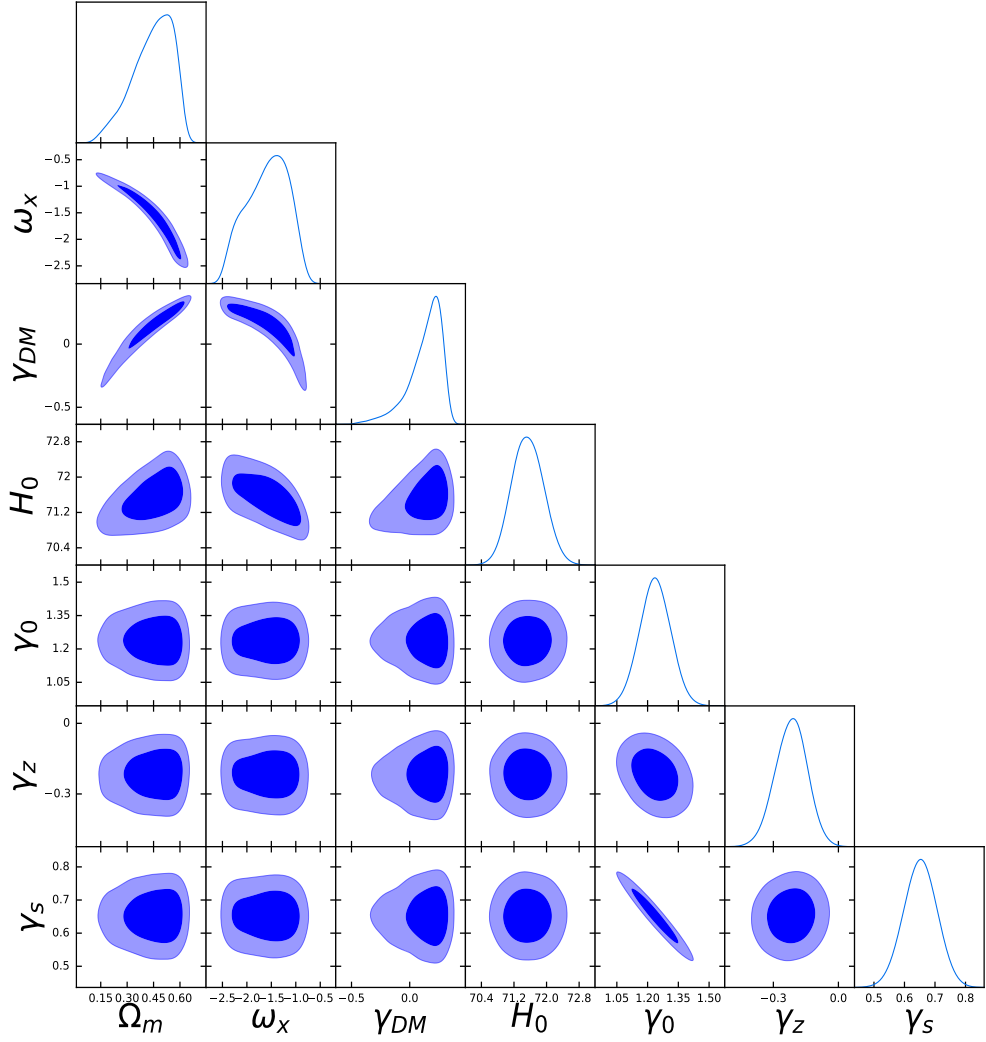


Figure 2. The 2D contour line obtained by using SGL+SNe+Hz.

We can see that the interaction factor γ_{DM} ($\gamma_{DM} = 0.134^{+0.17}_{-0.069}$) is not zero within the 1σ error range and the best value is also $\gamma_{DM} > 0$ from the Table. 1, which indicate there is a trend of conversion from DE to DM. The coincidence problem may be alleviated slightly at the range of 1σ error. In addition, the best value of H_0 is $H_0 = 71.54 \text{ kms}^{-1}\text{Mpc}^{-1}$, which is larger than $H_0 = 67.4 \text{ kms}^{-1}\text{Mpc}^{-1}$ given by Planck2018 [8] and smaller than $H_0 = 74.03 \text{ kms}^{-1}\text{Mpc}^{-1}$ given by Pantheon [64], which alleviates the conflict problem of H_0 to some extent. It shows that γ_{DM} model has the ability to alleviate the tension problem of Hubble constant H_0 which is consistent with the results in reference [65]. We also note that the coupling parameter γ_{DM} is correlated with all other model parameters Ω_m , ω_X and H_0 , and the cosmological constant model (Λ CDM) ($\gamma_{DM} = 0$, $\omega_X = 0$) is contained in the 2σ

confidence region. The matter density parameter Ω_m is also consistent with the result from other observable data in the 2σ confidence region [8, 64] although the best value is slightly larger.

5.3 WIMP DM relic density

In this part, we will show the calculation technique in detail for the scalar DM thermal average annihilation cross section that is the important component of the scalar DM relic density, which can be written as [66]:

$$\langle\sigma v\rangle=\frac{x}{8m_S^5K_2^2(x)}\int_{4m_S^2}^{\infty}(s-4m_S^2)\sqrt{s}K_1(x\sqrt{s}/m_S)\sigma ds. \quad (5.7)$$

Here $x=m_S/T$ (T is the temperature), $K_1(y)$ and $K_2(y)$ are the modified Bessel function of second kind, and s is the square of the center-of-mass energy. According to the our scalar DM model Eq. (5.1), there are four kinds of annihilation feynman diagrams which are shown in the Fig. 5.3, then scalar dark matter annihilation cross section σ can be obtained as,

$$\sigma=\sigma^{f\bar{f}}+\sigma^{W^+W^-}+\sigma^{ZZ}+\sigma^{hh}. \quad (5.8)$$

The cross section σ^{XX} can be cast into the following form:

$$\sigma^{XX}=\lambda_{hS}^2\nu^2|D_h(s)|^2\Gamma_{h\rightarrow XX}(s), \quad (5.9)$$

where,

$$|D_h(s)|^2\equiv\frac{1}{(s-m_h^2)^2+m_h^2\Gamma_h^2}. \quad (5.10)$$

After utilizing the standard quantum field theory calculations, the cross section in right hands of Eq. (5.8) can be obtained. More explicitly, we give the final result as follows:

$$\sigma^{f\bar{f}}=N_C^f\sum_f\frac{\lambda_{hS}^2m_f^2(1-4m_f^2/s)^{3/2}}{8\pi(m_h^2\Gamma_h^2+(s-m_h^2)^2)}, \quad (5.11)$$

$$\sigma^{W^+W^-}=\frac{\lambda_{hS}^2\left(s+12\frac{m_W^4}{s}-4m_W^2\right)\sqrt{1-4m_W^2/s}}{16\pi(m_h^2\Gamma_h^2+(s-m_h^2)^2)}, \quad (5.12)$$

$$\sigma^{ZZ}=\frac{\lambda_{hS}^2\left(s+12\frac{m_Z^4}{s}-4m_Z^2\right)\sqrt{1-4m_Z^2/s}}{32\pi(m_h^2\Gamma_h^2+(s-m_h^2)^2)}, \quad (5.13)$$

$$\sigma^{hh}=\frac{9\lambda_{hS}^2m_h^4\sqrt{1-4m_h^2/s}}{32\pi s(m_h^2\Gamma_h^2+(s-m_h^2)^2)}. \quad (5.14)$$

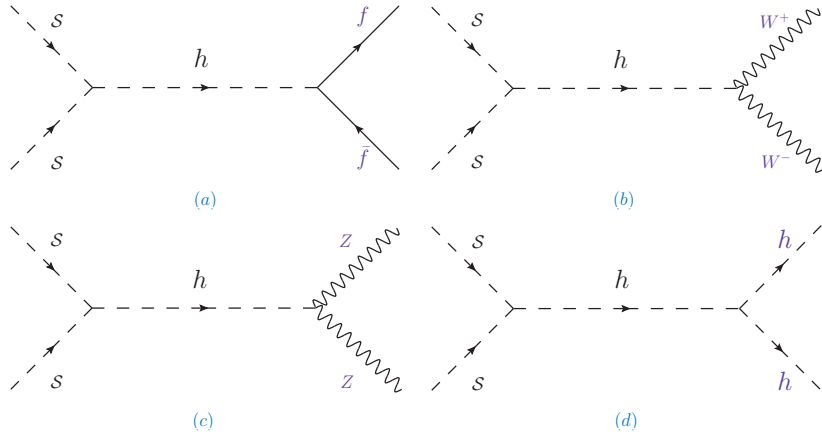


Figure 3. Feynman diagrams for the scalar dark matter annihilation.

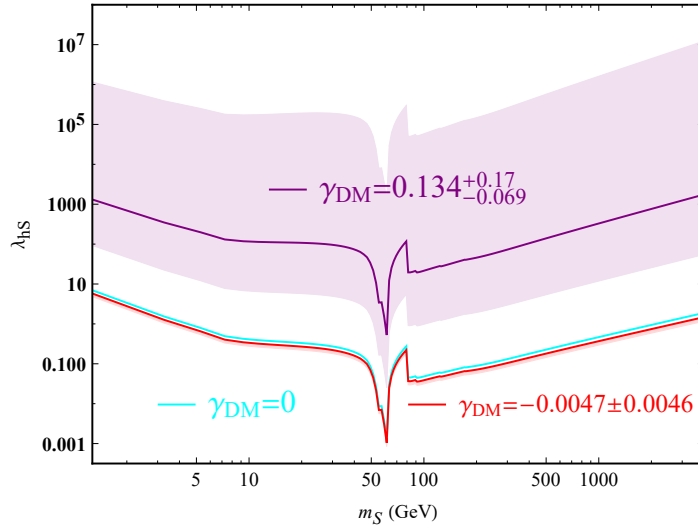


Figure 4. Allowed parameter regions in the $(m_S - \lambda_{hS})$ plane under the constraint of dark matter relic density $\Omega h^2 = 0.1198 \pm 0.0012$ [8].

These analytic annihilation formulas indicate that s must be more than twice the mass of a particle before the corresponding annihilation channel can be opened. For example, if $2m_W > s > 2m_{f\bar{f}}$, then only $\mathcal{S}\mathcal{S} \rightarrow f\bar{f}$ annihilation will be opened.

The newest Planck and WMAP data have measured the DM relic density in high precision [8]:

$$\Omega h^2 = 0.1198 \pm 0.0012. \quad (5.15)$$

For this scalar DM model, one can straightforward to get the scalar DM relic density by

inserting Eq. (5.7) into Eq. (4.6). We find that only the DM mass m_S , the coupling strength γ_{DM} and the coupling constant λ_{hS} are sensitive to the scalar DM relic density.

We show the allowed parameter regions in the $(m_S - \lambda_{hS})$ plane in the Fig. 5.3, where the bounded come from the DM relic density Eq. (5.15). In which, the cyan shad bands represent $\gamma_{DM} = 0$ that means there is a vanishing interaction between DE and scalar DM. The purple shad bands represent $\gamma_{DM} = 0.134^{+0.17}_{-0.069}$ case which is obtained from the (SGL+SNe+Hz) cosmological observations bounds. In other words, there is an interaction between DE and scalar DM, and the energy of DE convert into that of the scalar DM. And λ_{hS} decreases compared to the $\gamma_{DM} = 0$ case when scalar DM relic density limit is taken into account.

The red shad bands represent the case of $\gamma_{DM} = -0.0047 \pm 0.0046$ that is obtained by the limitation of the cosmological observation amount (GRBs+SNe+BAO+CMB). The negative coupling γ_{DM} means not only there is an interaction between DE and DM but also the energy of DM flows to that of the DE. After taking into account the limitation of the relic density of DM, λ_{hS} will be increased compared with the vanishing interaction scenario. The coupling of Higgs and scalar DM λ_{hS} is too large to be reasonable and even is excluded completely, which can also be seen from Fig. 5.3.

It should be emphasized that although the γ_{DM} obtained by the cosmological observation of (SGL+SNe+Hz) is large and beyond the range of x_f that set in the previous section, we found that in this case, x_f still remains around 20.

All the solid lines here represent the central values.

In addition, we can see that when all the lines have a obvious jump at $m_s \approx 80$ GeV, the reason is that the $\mathcal{SS} \rightarrow W^+W^-$ channel annihilation be opened when $s > 2m_W$. The contribution of this annihilation channel is larger and the discontinuity is very obvious. In fact, there will be a break in the lines as long as a channel is closed, which is not obvious due to the little difference contribution between adjacent channels.

5.4 DM direct detection

The spin-independent DM-nucleon scattering cross section for the scalar DM model has the form of [67]:

$$\sigma_{\text{SI}} = \frac{\lambda_{hS}^2 f_N^2 \mu^2 m_N^2}{4\pi m_h^4 m_S^2}, \quad (5.16)$$

where the DM-nucleon reduced mass $\mu = m_N m_S / (m_N + m_S)$ with m_N being the nucleon mass, the Higgs mass $m_h = 125$ GeV [68, 69], the hadron matrix element $f_N \simeq 0.3$ [70]. m_S and λ_{hS} are the DM mass and the coupling constant respectively, which depend on the constructed scalar DM model.

The spin-independent DM-nucleon mesh cross section as a function with m_S is shown in Fig. 5.4. The limitations of the direct DM detection experiments include LUX2015, LUX2016, XENON1T, which are marked by the magenta dashed, green the shaded bands, and blue dot-dashed line, respectively. While the cyan, red, and purple shaded bands are the $\gamma_{DM} = 0$, $\gamma_{DM} = -0.0047 \pm 0.0046$ and $\gamma_{DM} = 0.134^{+0.17}_{-0.069}$ cases, respectively.

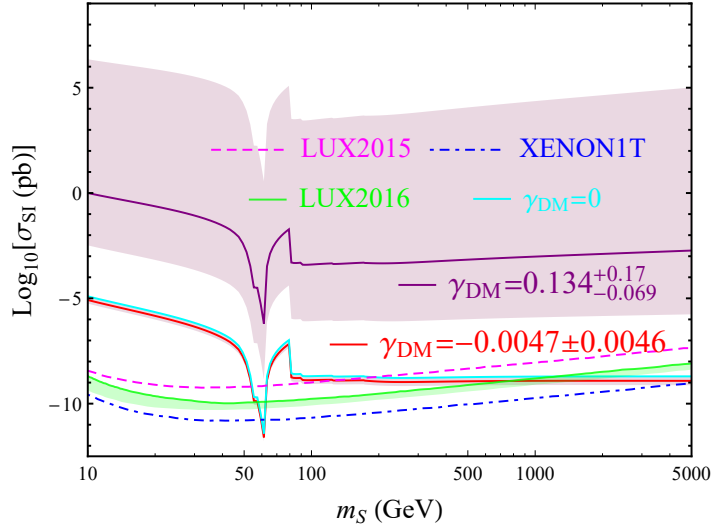


Figure 5. DM-nucleon scattering cross section σ_{SI} as the function of DM mass for several γ_{DM} . The magenta dashed line, purple line, and blue dot-dashed line represent the bounds from the LUX2015 [71], LUX2016 [71] and Xenon1T [71], respectively. And the purple shaded band refers to 2σ deviation to their central values that were chosen by authors in Ref. [67, 72].

Compared with $\gamma_{DM} = 0$, i.e., the DM and DE have vanishing interaction, Fig. 5.4 indicates that:

- When $\gamma_{DM} = 0.134^{+0.17}_{-0.069}$, the feasible parameter spaces of spin-independent DM-nucleon cross section shifts upward, after considering both the direct detection experiments and the DM relic density bounds, the scalar DM model will be completely eliminated.
- When $\gamma_{DM} = -0.0047 \pm 0.0046$, the shape will be shifted downward. Also, after taking into account the direct detection experiment and DM relic density limitation, the feasible parameter space of the scalar DM model is increased.

For example, under the limitation of LUX2016 experiment [71], the increase is not obvious in the resonant mass region, but it is relatively obvious in the large mass regions. More specifically, it can be obtained from Table. 2.

Therefore, if (SGL+SNe+Hz) and (GRBs+SNe+BAO+CMB) cosmological observation data are completely credible within the errors, but they lead to a completely contradictory conclusion, then the scalar DM model may have something wrong. On the contrary, if the scalar DM dark matter model is correct, then there must be something wrong for the (SGL+SNe+Hz) experimental data, while the correctness of the (GRBs+SNe+BAO+CMB) cosmological observation data need to be further confirmed.

Viable regions	Resonant mass regions	High mass regions
$\gamma_{DM} = 0.134^{+0.17}_{-0.069}$	—	—
$\gamma_{DM} = 0$	$59 \text{ GeV} \lesssim m_S \lesssim 63 \text{ GeV}$	$m_S \gtrsim 1.5 \text{ TeV}$
$\gamma_{DM} = -0.0047 \pm 0.0046$	$58 \text{ GeV} \lesssim m_S \lesssim 63 \text{ GeV}$	$m_S \gtrsim 0.8 \text{ TeV}$

Table 2. The viable regions in the resonant mass and high mass regions under the limits of LUX2016 for the three γ_{DM} cases [71].

6 Summary

In this paper, motivated by the simplest interaction model between DE and DM with interaction term $Q = 3\gamma_{DM}H\rho_{DM}$, we construct the corresponding interaction model of DE and WIMP DM. We then discuss the freeze-out parameter $x_f = m_{DM}/T$ with T being the DM freeze-out temperature and deduced the WIMP DM relic density in this new scenario. The resultant DM relic density will be magnified by $\frac{2-3\gamma_{DM}}{2}[2\pi g_* m_{DM}^3/(45s_0 x_f^3)]^{\gamma_{DM}}$ times, which open a new way to test WIMP DM models through the interaction strength γ_{DM} by using the constraints of observable data in cosmology.

For the interaction strength γ_{DM} , we employ cosmological observations to constrain the interaction strength γ_{DM} and find that different observations may make a significant difference for the interaction strength γ_{DM} . Specifically, (SGL+SNe+Hz) and (GRBs+SNe+BAO+CMB) cosmological observation data will give out $\gamma_{DM} = 0.134^{+0.17}_{-0.069}$ and $\gamma_{DM} = -0.0047 \pm 0.0046$ respectively. Note that it will vanish and reduce to the standard Λ CDM model when the interaction strength is $\gamma_{DM} = 0$.

As an example, we analyze the case where WIMP DM is a scalar DM. After further considering the constraints from the DM direct detection experiment and DM relic density, we observe that the allowed parameter space of the scalar DM model will be completely excluded for (SGL+SNe+Hz) cosmological observation data, while it will be increased for (GRBs+SNe+BAO+CMB) cosmological observation data. Those two cosmological observation data lead to a paradoxical conclusion. Thus, more accurate predictions for γ_{DM} based on the cosmological observations data will provide us with a possible way to screen the WIMP DM models.

Acknowledgement: We are grateful to Prof. Yu-Feng Zhou for helpful communications and discussions. This work was supported in part by Graduate Research and Innovation Foundation of Chongqing, China (Grant No. CYS20272), the China Postdoctoral Science Foundation under Grant No. (2019TQ0329, 2020M670476), and the National Natural Science Foundation of China under Grant No.11947302. Jia-Wei Zhang was supported by the Natural Science Foundation of Chongqing under Grants No. cstc2018jcyjAX0713, the Science and Technology Research Program of Chongqing Municipal Education Commission under Grant No. KJQN202001541, and the Research Foundation of Chongqing University of Science and

Technology under Grant No. CK2016Z03.

References

- [1] G. R. Blumenthal, S. M. Faber, J. R. Primack and M. J. Rees, “Formation of Galaxies and Large Scale Structure with Cold Dark Matter,” *Nature* **311**, 517-525 (1984)
- [2] M. Davis, G. Efstathiou, C. S. Frenk and S. D. M. White, “The Evolution of Large Scale Structure in a Universe Dominated by Cold Dark Matter,” *Astrophys. J.* **292**, 371-394 (1985)
- [3] D. Clowe, M. Bradac, A. H. Gonzalez, M. Markevitch, S. W. Randall, C. Jones and D. Zaritsky, “A direct empirical proof of the existence of dark matter,” *Astrophys. J. Lett.* **648**, L109-L113 (2006)
- [4] A. G. Riess *et al.* [Supernova Search Team], “Observational evidence from supernovae for an accelerating universe and a cosmological constant,” *Astron. J.* **116**, 1009-1038 (1998)
- [5] S. Perlmutter *et al.* [Supernova Cosmology Project], “Measurements of Ω and Λ from 42 high redshift supernovae,” *Astrophys. J.* **517**, 565-586 (1999)
- [6] C. L. Bennett *et al.* [WMAP], “Nine-Year Wilkinson Microwave Anisotropy Probe (WMAP) Observations: Final Maps and Results,” *Astrophys. J. Suppl.* **208**, 20 (2013)
- [7] P. A. R. Ade *et al.* [Planck], “Planck 2015 results. XIII. Cosmological parameters,” *Astron. Astrophys.* **594**, A13 (2016)
- [8] N. Aghanim *et al.* [Planck], “Planck 2018 results. VI. Cosmological parameters,” *Astron. Astrophys.* **641**, A6 (2020)
- [9] C. O. Heinke, A. Bahramian, N. Degenaar and R. Wijnands, “The nature of very faint X-ray binaries; hints from light curves,” *Mon. Not. Roy. Astron. Soc.* **447**, 3034 (2015)
- [10] T. Bringmann, X. Huang, A. Ibarra, S. Vogl and C. Weniger, “Fermi LAT Search for Internal Bremsstrahlung Signatures from Dark Matter Annihilation,” *JCAP* **07**, 054 (2012)
- [11] C. Weniger, “A Tentative Gamma-Ray Line from Dark Matter Annihilation at the Fermi Large Area Telescope,” *JCAP* **08**, 007 (2012)
- [12] O. Macias, S. Horiuchi, M. Kaplinghat, C. Gordon, R. M. Crocker and D. M. Nataf, “Strong Evidence that the Galactic Bulge is Shining in Gamma Rays,” *JCAP* **09**, 042 (2019)
- [13] M. Ackermann *et al.* [Fermi-LAT], “Measurement of separate cosmic-ray electron and positron spectra with the Fermi Large Area Telescope,” *Phys. Rev. Lett.* **108**, 011103 (2012)
- [14] E. Aprile [XENON1T], “The XENON1T Dark Matter Search Experiment,” *Springer Proc. Phys.* **148**, 93-96 (2013)
- [15] D. S. Akerib *et al.* [LUX], “First results from the LUX dark matter experiment at the Sanford Underground Research Facility,” *Phys. Rev. Lett.* **112**, 091303 (2014)
- [16] D. S. Akerib *et al.* [LUX], “Results from a search for dark matter in the complete LUX exposure,” *Phys. Rev. Lett.* **118**, no.2, 021303 (2017)
- [17] A. Tan *et al.* [PandaX-II], “Dark Matter Results from First 98.7 Days of Data from the PandaX-II Experiment,” *Phys. Rev. Lett.* **117**, no.12, 121303 (2016)
- [18] K. Fujii *et al.*, “Physics Case for the International Linear Collider,”

- [19] M. Bicer *et al.* [TLEP Design Study Working Group], “First Look at the Physics Case of TLEP,” JHEP **1401**, 164 (2014)
- [20] D. d’Enterria, “Physics at the FCC-ee,”
- [21] CEPC-SPPC Study Group, “CEPC-SPPC Preliminary Conceptual Design Report. 1. Physics and Detector,” IHEP-CEPC-DR-2015-01, IHEP-TH-2015-01, IHEP-EP-2015-01.
- [22] W. Zimdahl and D. Pavon, “Interacting quintessence,” Phys. Lett. B **521**, 133-138 (2001)
- [23] C. Feng, B. Wang, E. Abdalla and R. K. Su, “Observational constraints on the dark energy and dark matter mutual coupling,” Phys. Lett. B **665**, 111-119 (2008)
- [24] B. Wang, J. Zang, C. Y. Lin, E. Abdalla and S. Micheletti, “Interacting Dark Energy and Dark Matter: Observational Constraints from Cosmological Parameters,” Nucl. Phys. B **778**, 69-84 (2007)
- [25] B. Wang, Y. g. Gong and E. Abdalla, “Transition of the dark energy equation of state in an interacting holographic dark energy model,” Phys. Lett. B **624**, 141-146 (2005)
- [26] J. Cui and X. Zhang, “Cosmic age problem revisited in the holographic dark energy model,” Phys. Lett. B **690**, 233-238 (2010)
- [27] E. Abdalla and B. Wang, “The Mass and the coupling of the dark particle,” Phys. Lett. B **651**, 89-91 (2007)
- [28] M. Jamil and M. A. Rashid, “Interacting Dark Energy with Inhomogeneous Equation of State,” Eur. Phys. J. C **56**, 429-434 (2008)
- [29] O. Bertolami, F. Gil Pedro and M. Le Delliou, “Dark Energy-Dark Matter Interaction and the Violation of the Equivalence Principle from the Abell Cluster A586,” Phys. Lett. B **654**, 165-169 (2007)
- [30] M. Szydlowski, “Cosmological model with energy transfer,” Phys. Lett. B **632**, 1-5 (2006)
- [31] Y. Chen, Z. H. Zhu, J. S. Alcaniz and Y. Gong, “Using A Phenomenological Model to Test the Coincidence Problem of Dark Energy,” Astrophys. J. **711**, 439-444 (2010)
- [32] S. Cao, N. Liang and Z. H. Zhu, “Testing the phenomenological interacting dark energy with observational $H(z)$ data,” Mon. Not. Roy. Astron. Soc. **416**, 1099-1104 (2011)
- [33] H. Zhang, H. Yu, Z. H. Zhu and Y. Gong, “A quantitative criteria for the coincidence problem,” Phys. Lett. B **678**, 331-334 (2009)
- [34] Y. Zhang and H. Li, “A New Type of Dark Energy Model,” JCAP **06**, 003 (2010)
- [35] S. Kumar and R. C. Nunes, “Observational constraints on dark matter–dark energy scattering cross section,” Eur. Phys. J. C **77**, no.11, 734 (2017)
- [36] W. Yang, S. Pan, E. Di Valentino, R. C. Nunes, S. Vagnozzi and D. F. Mota, “Tale of stable interacting dark energy, observational signatures, and the H_0 tension,” JCAP **09**, 019 (2018)
- [37] E. Di Valentino, A. Melchiorri, O. Mena and S. Vagnozzi, “Interacting dark energy in the early 2020s: A promising solution to the H_0 and cosmic shear tensions,” Phys. Dark Univ. **30**, 100666 (2020)
- [38] E. Di Valentino, A. Melchiorri, O. Mena and S. Vagnozzi, “Nonminimal dark sector physics and cosmological tensions,” Phys. Rev. D **101**, no.6, 063502 (2020)

- [39] Y. Pan, S. Cao, Y. Gong, K. Liao and Z. H. Zhu, “Testing the interaction model with cosmological data and gamma-ray bursts,” *Phys. Lett. B* **718**, 699-703 (2013)
- [40] S. Cao, Y. Chen, J. Zhang and Y. Ma, “Testing the Interaction Between Baryons and Dark Energy with Recent Cosmological Observations,” *Int. J. Theor. Phys.* **54**, no.5, 1492-1505 (2015)
- [41] J. J. Cao, Z. X. Heng, J. M. Yang, Y. M. Zhang and J. Y. Zhu, “A SM-like Higgs near 125 GeV in low energy SUSY: a comparative study for MSSM and NMSSM,” *JHEP* **03**, 086 (2012)
- [42] Q. H. Cao, E. Ma and G. Rajasekaran, “Observing the Dark Scalar Doublet and its Impact on the Standard-Model Higgs Boson at Colliders,” *Phys. Rev. D* **76**, 095011 (2007)
- [43] Y. Gao, T. Ghosh, K. Sinha and J. H. Yu, “SU(2) \times SU(2) \times U(1) interpretations of the diboson and Wh excesses,” *Phys. Rev. D* **92**, no.5, 055030 (2015)
- [44] H. Terazawa and M. Yasue, “Excited Gauge and Higgs Bosons in the Unified Composite Model,” *Nonlin. Phenom. Complex Syst.* **19**, no.1, 1-6 (2016)
- [45] X. Liu and Z. Liu, “TeV dark matter and the DAMPE electron excess,” *Phys. Rev. D* **98**, no.3, 035025 (2018)
- [46] J. Yepes, “Top partners tackling vector dark matter,” *Phys. Lett. B* **811**, 135890 (2020)
- [47] V. Silveira and A. Zee, “SCALAR PHANTOMS,” *Phys. Lett. B* **161**, 136-140 (1985)
- [48] J. McDonald, “Gauge singlet scalars as cold dark matter,” *Phys. Rev. D* **50**, 3637-3649 (1994)
- [49] C. P. Burgess, M. Pospelov and T. ter Veldhuis, “The Minimal model of nonbaryonic dark matter: A Singlet scalar,” *Nucl. Phys. B* **619**, 709-728 (2001)
- [50] V. Barger, P. Langacker, M. McCaskey, M. J. Ramsey-Musolf and G. Shaughnessy, “LHC Phenomenology of an Extended Standard Model with a Real Scalar Singlet,” *Phys. Rev. D* **77**, 035005 (2008)
- [51] M. Gonderinger, Y. Li, H. Patel and M. J. Ramsey-Musolf, “Vacuum Stability, Perturbativity, and Scalar Singlet Dark Matter,” *JHEP* **01**, 053 (2010)
- [52] H. Han, J. M. Yang, Y. Zhang and S. Zheng, “Collider Signatures of Higgs-portal Scalar Dark Matter,” *Phys. Lett. B* **756**, 109-112 (2016)
- [53] H. Wu and S. Zheng, “Scalar Dark Matter: Real vs Complex,” *JHEP* **03**, 142 (2017)
- [54] C. Boehm, X. Chu, J. L. Kuo and J. Pradler, “Scalar Dark Matter Candidates – Revisited,”
- [55] Y. Pan, S. Cao and L. Li, “Constraints on interacting dark energy from time delay lenses,” *Int. J. Mod. Phys. D* **25**, no.01, 1650003 (2015)
- [56] Y. Chen, S. Kumar, B. Ratra, “Planck 2018 results. VI. Cosmological parameters,” *MNRAS* **488**, 3745 (2019)
- [57] J. J. Wei, X. F. Wu “Planck 2018 results. VI. Cosmological parameters,” *APJ* **838**, 160(2017)
- [58] D. M. Scolnic, D. O. Jones, A. Rest *et al.*, “Planck 2018 results. VI. Cosmological parameters,” *APJ* **859**, 101(2018)
- [59] M. W. Auger, T. Treu, A. S. Bolton *et al.*, “Planck 2018 results. VI. Cosmological parameters,” *APJ* **724**, 1 (2010)

- [60] M. Cappellari, R. Bacon, M. Bureau *et al.*, “Planck 2018 results. VI. Cosmological parameters,” MNRAS **366**, 1126-1150 (2006)
- [61] I. Jorgensen, M. Franx, P. Kjaergaard, “Planck 2018 results. VI. Cosmological parameters,” MNRAS **276**, 4 (1995)
- [62] <http://hitoshi.berkeley.edu/229C/index.html>
- [63] A. Lewis, S. Bridle, Phys. Rev. D **66** (2002) 103511
- [64] A. G. Riess, S. Casertano, W. L. Yuan *et al.* “Planck 2018 results. VI. Cosmological parameters,” APJ. **876**, 85 (2019)
- [65] X. Zheng, M. Biesiada, S. Cao, J. Qi and Z. H. Zhu, “Ultra-compact structure in radio quasars as a cosmological probe: a revised study of the interaction between cosmic dark sectors,” JCAP **10**, 030 (2017)
- [66] P. Gondolo and G. Gelmini, “Cosmic abundances of stable particles: Improved analysis,” Nucl. Phys. B **360**, 145-179 (1991)
- [67] X. G. He and J. Tandean, “New LUX and PandaX-II Results Illuminating the Simplest Higgs-Portal Dark Matter Models,” JHEP **12**, 074 (2016)
- [68] G. Aad *et al.* [ATLAS], “Observation of a new particle in the search for the Standard Model Higgs boson with the ATLAS detector at the LHC,” Phys. Lett. B **716**, 1-29 (2012)
- [69] S. Chatrchyan *et al.* [CMS], “Observation of a New Boson at a Mass of 125 GeV with the CMS Experiment at the LHC,” Phys. Lett. B **716**, 30-61 (2012)
- [70] J. M. Cline, K. Kainulainen, P. Scott and C. Weniger, “Update on scalar singlet dark matter,” Phys. Rev. D **88**, 055025 (2013)
- [71] E. Aprile *et al.* [XENON], “Physics reach of the XENON1T dark matter experiment,” JCAP **04**, 027 (2016)
- [72] M. Escudero, A. Berlin, D. Hooper and M. X. Lin, “Toward (Finally!) Ruling Out Z and Higgs Mediated Dark Matter Models,” JCAP **12**, 029 (2016)